

A semi-analytical method for predicting the performance and convergence behavior of a multi-user turbo-equalizer/demapper

Valéry Ramon*, Cédric Herzet, Luc Vandendorpe

Communications and Remote Sensing Laboratory, Université catholique de Louvain (UCL)
2, place du Levant, B-1348 Louvain-la-Neuve, Belgium
{ramon, herzet, vandendorpe}@tele.ucl.ac.be

Abstract—This paper proposes a simple semi-analytical method with reduced simulation time for predicting at any iteration the performance of a turbo-equalization/demapping scheme using the Wang and Poor soft-in/soft-out (SISO) Minimum Mean Square Error (MMSE) / Interference Cancellation (IC) equalizer and a SISO decoder. The proposed method may be applied to multi-level/phase data modulations as well as multi-user context. This paper shows that the equalizer behavior may be very reliably predicted totally by calculations (no simulations are needed) whereas that of the decoder still requires simulations. Comparison between the proposed prediction method and plain simulations of the overall turbo equalization scheme demonstrates that our method accurately determines the system performance at any iteration. Static channels, long frames and perfect channel knowledge are assumed throughout the paper.

I. INTRODUCTION

Turbo-equalization/demapping (references in [1]) is a powerful mean to perform joint equalization/demapping and decoding when considering coded data transmission over frequency selective channels. The association of the code and the discrete-time equivalent channel (separated by an interleaver) may be regarded as the serial concatenation of two codes. The turbo principle may then be used at the receiver : the system performance measured in terms of the bit error rate (BER) is improved through the exchange of extrinsic information between a soft-in/soft-out (SISO) equalizer/demapper and a SISO decoder.

The goal of this paper is to predict the performance and convergence behavior of such a turbo-equalization/demapping scheme at any iteration using a simple semi-analytical method. The intention is to replace simulations of some part of the receiver chain, namely the equalizer, by calculations. The proposed prediction method may be applied to multi-level/phase data modulations as well as multi-user contexts. Nevertheless, for the sake of clarity, only simple cases will be considered in this paper. Three cases of gradually increasing difficulty, namely single-user Binary Phase-Shift Keying (BPSK), single-user Quadrature Phase-Shift Keying (QPSK) and multi-user BPSK, will thus be successively developed. This way to proceed will ease understanding and enable to point out the slight differences between these various cases. The SISO Minimum

Mean Square Error (MMSE) / Interference Cancellation (IC) equalizer/demapper which will be analyzed in this paper is the one proposed by Wang and Poor [2] for BPSK data modulation and multi-user context. This multiuser equalizer is suboptimal but it exhibits reasonable complexity while offering interesting performance [2]. It was extended notably in [1] to multi-level/phase data modulation, in [3] to multiple-input multiple-output (MIMO) systems and simplified in [4] in order to deal with time-invariant equalizer coefficients. It is more particularly this latter version which will be analyzed in the present paper. However, an extension of the proposed prediction method to other linear equalizers using a priori information on data symbols is straightforward. A SISO convolutional decoder using the BCJR algorithm [5] will be considered in the sequel although other SISO decoders (low-density parity check (LDPC) decoder, ...) might also be used.

Various methods for predicting the convergence behavior of turbo decoding schemes as well as parallel or serially ([6] and references therein, [7] and references therein) concatenated codes have been previously proposed. They are based e.g. on variance or signal-to-noise ratio transfer analysis or extrinsic information transfer chart (EXIT chart). Almost all of them require simulations letting vary at least one input parameter for each of the two devices involved in the turbo process. To our knowledge, the only papers which propose calculations rather than simulations for some parts of the receiver chain are [8], [9] and [10]. Reference [8] found the error variance on the symbol estimates at the output of a parallel interference canceller assuming gaussianity of the non-cancelled multi-user interference. Reference [9] used the so-called unscented transformation for calculating the mean of the Log-Likelihood Ratios (LLRs) output by the MMSE/IC equalizer. Nevertheless, this approach has been developed only in the single-user BPSK case and is a little more complex than the one described in this paper. Reference [9] also calculated the probability density function (pdf) of the extrinsic LLRs delivered by a LDPC decoder assuming a mixture of Gaussian pdf for the decoder input LLRs distribution. Reference [10] presented an optimal iterative multiuser detector/decoder based on cross-entropy minimization techniques as well as a practical implementation of this algorithm. A theoretical analysis showed that, with this approach, multiuser detection/decoding is capable of achieving optimal single-user performance for

Valéry Ramon would like to thank the Belgian NSF for its financial support. This research is partly funded by the Federal Office for Scientific, Technical and Cultural Affairs (OSTC, Belgium) through the IAP contract No P5/11.

user correlations approaching one. For our part, we already presented in [11] an overview of the prediction method developed hereafter but only in the single-user BPSK case.

The prediction method proposed in this paper requires simulations only of the decoder. Indeed, as we will show in the sequel, the equalizer/demapper behavior may be accurately and totally predicted by calculations (so without any simulation) using simplifying approximations. In other words, the input/output relations of the equalizer/demapper may be given analytically. One of these approximations is the gaussianity of the extrinsic LLRs output by the equalizer/demapper as well as the decoder. The impact of these Gaussian assumptions on the performance of our prediction method will be illustrated.

The gaussianity of the LLRs computed by the constituent stages of the receiver is a hypothesis made in all the hereabove cited papers. Reference [7] provides theoretical justification for the Gaussian approximation in turbo decoding when the frame length becomes very large. Reference [12] shows that this assumption is accurate for sum-product decoding algorithms in the general setup of decoding of graph-based codes. References [4] and [6], when drawing their EXIT charts respectively for turbo-equalization and parallel concatenated codes, used this assumption which turned out to be accurate enough for predicting the system convergence behavior. The reliability of this hypothesis may also be illustrated by simulation results.

If the decoder may be simulated in advance for some fixed parameters (constraint length, code rate,...), our method enables to foretell the performance and convergence behavior of the equalized system given that decoder, without further simulations, for any frequency selective channel and at any E_b/N_0 . Performance with the reference additive white Gaussian noise (AWGN) channel or with perfect knowledge of a priori information at the equalizer input may then also be directly obtained.

In the single-user BPSK case, the proposed method for calculating the equalizer/demapper behavior will significantly reduce the number of simulations needed to establish the EXIT chart [4]. Indeed, we are now able to calculate (rather than simulate) the equalizer characteristic curves for any channel and any E_b/N_0 . Simulations remain necessary only for drawing the decoder characteristic curve.

Static channels, long frames and perfect channel knowledge at the receiver will be assumed throughout the paper.

The sequel of this paper will be organized as follows. Section II will introduce the system model. Our method for predicting the performance of the turbo-equalization/demapping scheme will be explained in section III. This section will successively consider single-user BPSK, single-user QPSK and multi-user BPSK cases. Section IV will compare for different channels the performance obtained with our prediction method to that obtained by plain simulations of the turbo-equalizer/demapper. It will be observed that our method accurately determines the system performance at any iteration.

II. SYSTEM MODEL

In this section, the transmitter model (subsection II-A), the overall iterative receiver (subsection II-B) and the equations

of the considered MMSE/IC equalizer (subsection II-C) will be successively presented for the most general case : K users propagating through frequency-selective channels and using multi-level/phase data modulation. As no novelty is introduced with respect to the equalizer of [1], [2] and [4], only the equations which will be useful for section III will be given.

A. Transmitter model

Let us consider a K -user convolutionally coded Direct-Sequence Code Division Multiple Access (DS-CDMA) communication system with spreading factor M . The block diagram of the transmitter-end is similar to [1] and [2] and is shown in Fig. 1. For any user k ($k = 1, \dots, K$), a frame of information bits $u_k(p)$ is encoded by a same rate- r convolutional encoder. The resulting encoded bits $b_k(n)$ are interleaved using a random permutation function to give the interleaved coded bits $b_k(l)$. These bits are then mapped onto symbols $s_k(i)$ ($i = 1, \dots, I$) belonging to some constellation alphabet \mathcal{A} . These symbols are modulated by a spreading waveform and transmitted over a frequency-selective channel, which is assumed to be static and perfectly known. Both the spreading waveform and the channel are specific to each user. At the receiver, after the summation of all the users signals and addition of the white gaussian noise, chip-matched filtering and chip-rate sampling are successively performed. Each k -th user composite channel may thus be represented by its equivalent discrete-time model. This one includes the effect of the k -th user spreading, the k -th user channel itself, the chip-matched filtering and the chip-rate sampling. It results in a causal discrete-time filter with chip-rate coefficients $h_k(jM + m)$ where $j = 0, \dots, L$ and $m = 0, \dots, M - 1$. $L + 1$ thus denotes the length of the channel impulse response expressed in number of symbols. The observations $r(iM + m)$ at the output of the channel may thus be expressed as

$$r(iM + m) = \sum_{k=1}^K \sum_{j=0}^L h_k(jM + m) s_k(i - j) + n(iM + m), \quad (1)$$

where $n(iM + m)$ are Gaussian noise samples of variance σ_n^2 .

B. Overall iterative receiver

The block scheme of the overall iterative receiver is illustrated in Fig. 2 and is more described in [1], [2] or [4]. It consists of two stages : a SISO multi-user equalizer/demapper followed by K parallel single-user SISO channel decoders. The two stages are separated by bit-deinterleavers and interleavers. They exchange extrinsic information, on iterative fashion, in order to improve the system performance. The channel code considered in the sequel is a convolutional code and decoding is implemented using the well-known BCJR algorithm. Nevertheless, other codes (e.g. LDPC code) and SISO decoding algorithms might be used.

C. MMSE/IC equalizer equations

Now that the overall iterative receiver has been quickly presented, let us focus more deeply on the MMSE/IC equalizer equations. These will be useful for understanding section III.

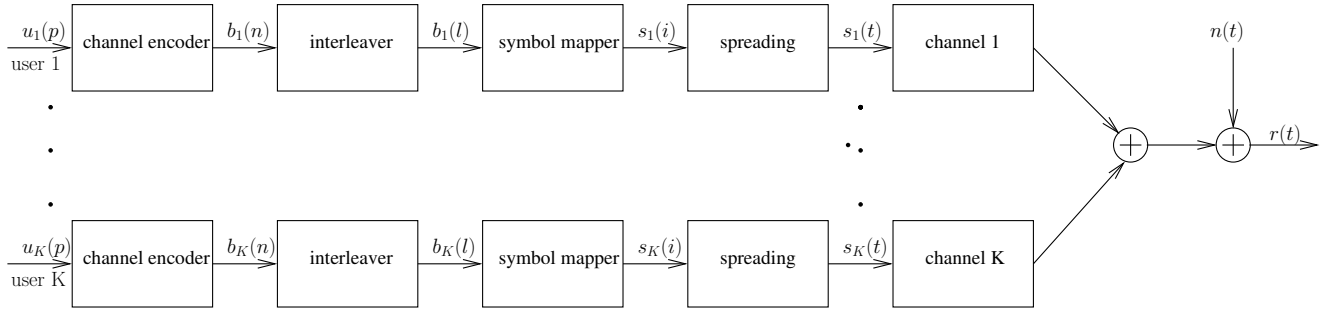


Fig. 1. Transmitter : convolutionally-coded DS-CDMA system with K users transmitting through a frequency-selective channel.

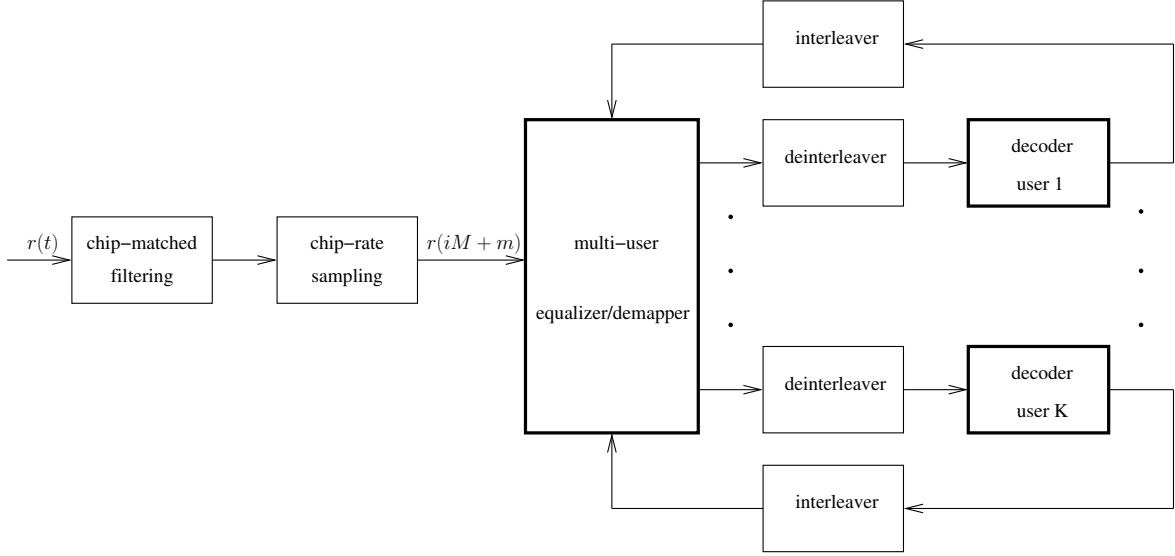


Fig. 2. Iterative receiver : soft-in soft-out (SISO) multi-user equalizer/demapper followed by K parallel single-user SISO channel decoders.

For $0 \leq j \leq L$, defining a $M \times K$ matrix

$$\underline{H}(j) = \begin{bmatrix} h_1(jM) & \dots & h_K(jM) \\ \vdots & \ddots & \vdots \\ h_1(jM + M - 1) & \dots & h_K(jM + M - 1) \end{bmatrix}$$

and the following vectors

$$\begin{aligned} \underline{r}(i) &\triangleq [r(iM) \ r(iM + 1) \ \dots \ r(iM + M - 1)]^T, \\ \underline{s}(i) &\triangleq [s_1(i) \ s_2(i) \ \dots \ s_K(i)]^T, \\ \underline{n}(i) &\triangleq [n(iM) \ n(iM + 1) \ \dots \ n(iM + M - 1)]^T, \end{aligned}$$

we may write

$$\underline{r}(i) = \sum_{j=0}^L \underline{H}(j) \underline{s}(i - j) + \underline{n}(i).$$

Defining the equalizer length as $N \triangleq N_1 + N_2 + 1$, we may introduce a sliding-window model using the following vectors

$$\begin{aligned} \mathbf{r}(i) &\triangleq [\underline{r}(i - N_1) \ \dots \ \underline{r}(i) \ \dots \ \underline{r}(i + N_2)]_{NM \times 1}^T, \\ \mathbf{s}(i) &\triangleq [\underline{s}(i - N_1 - L) \ \dots \ \underline{s}(i) \ \dots \ \underline{s}(i + N_2)]_{(N+L)K \times 1}^T, \\ \mathbf{n}(i) &\triangleq [\underline{n}(i - N_1) \ \dots \ \underline{n}(i) \ \dots \ \underline{n}(i + N_2)]_{NM \times 1}^T, \end{aligned}$$

and the $(MN \times (N + L)K)$ -channel matrix

$$\mathbf{H} = \begin{bmatrix} \underline{H}(L) & \dots & \underline{H}(0) & 0 & \dots & \dots & 0 \\ 0 & \underline{H}(L) & \dots & \underline{H}(0) & 0 & \dots & 0 \\ \vdots & \ddots & \ddots & \ddots & \ddots & \ddots & \vdots \\ 0 & \dots & \dots & 0 & \underline{H}(L) & \dots & \underline{H}(0) \end{bmatrix}. \quad (2)$$

This enables to write for each symbol time index i

$$\mathbf{r}(i) = \mathbf{H} \mathbf{s}(i) + \mathbf{n}(i), \quad (3)$$

where $\mathbf{n}(i) \sim \mathcal{N}_c(0, \sigma_n^2 \mathbf{I})$, \mathbf{I} being the $MN \times MN$ identity matrix. In the single-user case, the dimensionality of the preceding vectors and matrices significantly reduces since K and M are then both equal to 1 (spreading is not needed).

Let $\tilde{s}_k(i) \triangleq E\{s_k(i)\}$ and $\text{var}\{s_k(i)\} \triangleq E\{|s_k(i)|^2\} - |\tilde{s}_k(i)|^2$ denote respectively the so-called a priori mean (E stands for expectation) and variance of symbol $s_k(i)$ which are computed as explained in [1], [2] and [4] from the a priori LLRs at the equalizer input. For normalized PSK constellations, we have of course $E\{|s_k(i)|^2\} = 1 \ \forall k, i$.

Using the following definitions

$$\begin{aligned}
\tilde{\mathbf{s}}(i) &\triangleq [\tilde{s}_1(i) \dots \tilde{s}_K(i)]^T, \\
\tilde{\mathbf{s}}(i) &\triangleq [\tilde{\mathbf{s}}(i - N_1 - L)^T \dots \tilde{\mathbf{s}}(i)^T \dots \tilde{\mathbf{s}}(i + N_2)^T]^T, \\
\tilde{\mathbf{s}}_k(i) &\triangleq \tilde{\mathbf{s}}(i) - \tilde{s}_k(i) \mathbf{e}_k, \\
\mathbf{r}_{ss,k}(i+l) &\triangleq [\text{var}\{s_1(i+l)\} \dots \text{var}\{s_K(i+l)\}]^T \\
&\quad \text{for } l = -N_1 - L, \dots, -1, 1, \dots, N_2, \\
\mathbf{r}_{ss,k}(i) &\triangleq [\text{var}\{s_1(i)\} \dots \text{var}\{s_{k-1}(i)\}, 1, \\
&\quad \text{var}\{s_{k+1}(i)\}, \dots, \text{var}\{s_K(i)\}]^T, \\
\mathbf{R}_{ss,k}(i) &\triangleq \text{diag}[\mathbf{r}_{ss,k}(i - N_1 - L)^T \dots \mathbf{r}_{ss,k}(i)^T \\
&\quad \dots \mathbf{r}_{ss,k}(i + N_2)^T], \\
\mathbf{w}_k(i) &\triangleq [\mathbf{H}\mathbf{R}_{ss,k}(i)\mathbf{H}^H + \sigma_n^2\mathbf{I}]^{-1}\mathbf{H}\mathbf{e}_k,
\end{aligned} \tag{4}$$

the symbol estimate $\hat{s}_k(i)$ is given by

$$\hat{s}_k(i) = \mathbf{w}_k^H(i) [\mathbf{r}(i) - \mathbf{H}\tilde{\mathbf{s}}_k(i)], \tag{5}$$

where \mathbf{e}_k denotes a length- $(N+L)K$ vector of zeros except for the $((N_1+L)K+k)$ th element, which is 1.

An efficient approximation made in [4] - which is not used in [1] and [2] - leading to a complexity reduction of the equalizer and weak performance degradation may be obtained by computing for each user k the mean a priori variance over the I transmitted symbols in the k -th user frame

$$v_k \triangleq \frac{1}{I} \sum_{i=1}^I \text{var}\{s_k(i)\}. \tag{6}$$

Letting $\underline{v} = [v_1, v_2, \dots, v_K]^T$ and $\underline{v}_k = [v_1, \dots, v_{k-1}, 1, v_{k+1}, \dots, v_K]^T$, a matrix $\mathbf{R}_{ss,k} = \text{diag}[\underline{v}^T \dots \underline{v}^T \underline{v}_k^T \underline{v}_k^T \dots \underline{v}^T]$ which is independent of i (but still dependent on k) may thus be defined. Consequently $\mathbf{w}_k(i)$ calculated with $\mathbf{R}_{ss,k}$ instead of $\mathbf{R}_{ss,k}(i)$ does not depend on i either and will be denoted by \mathbf{w}_k . The equalizer complexity is thus reduced since the calculation of the equalizer coefficients \mathbf{w}_k by (4) - which requires a matrix inversion - has to be performed only once for each user and no longer for each symbol. We will use this approximation throughout the remainder of this paper.

Exactly as in [1], [2] and [4], we assume that the estimate $\hat{s}_k(i)$ provided by the equalizer is the output of an equivalent AWGN channel having $s_k(i)$ as its input i.e.

$$\hat{s}_k(i) = \mu_k s_k(i) + \nu_k(i) \tag{7}$$

where $\nu_k(i)$ is a complex noise and $\nu_k(i) \sim \mathcal{N}_c(0, \sigma_{\nu_k}^2)$. Parameters μ_k and $\sigma_{\nu_k}^2$ may be easily calculated as follows [2] :

$$\mu_k = \mathbf{w}_k^H \mathbf{H} \mathbf{e}_k, \tag{8}$$

$$\sigma_{\nu_k}^2 = \mu_k - \mu_k^2. \tag{9}$$

Finally, the equalizer outputs extrinsic LLRs on the interleaved coded bits $b_k(l)$ denoted by $L_e^{EQ}(b_k(l))$. Assuming that the bits characterizing symbol $s_k(i)$ are denoted by $b_k^p(i) = b_k((i-1)q+p)$ ($p = 1, \dots, q$ where q is the number of bits per symbol for the considered constellation \mathcal{A}) and that

they are independent from each other thanks to interleaving, $L_e^{EQ}(b_k^p(i))$ is given [1] by

$$\begin{aligned}
L_e^{EQ}(b_k^p(i)) &= \\
&\ln \frac{\sum_{s_k(i): b_k^p(i)=1} p(\hat{s}_k(i)|s_k(i)) \left[\prod_{\substack{r=1, \dots, q \\ r \neq p}} P_a(b_k^r(i)) \right]}{\sum_{s_k(i): b_k^p(i)=0} p(\hat{s}_k(i)|s_k(i)) \left[\prod_{\substack{r=1, \dots, q \\ r \neq p}} P_a(b_k^r(i)) \right]},
\end{aligned} \tag{10}$$

where

$$p(\hat{s}_k(i)|s_k(i)) = \frac{1}{\pi \sigma_{\nu_k}^2} \exp \left[-\frac{|\hat{s}_k(i) - \mu_k s_k(i)|^2}{\sigma_{\nu_k}^2} \right]. \tag{11}$$

$P_a(b_k^r(i))$ are the a priori probabilities on bits $b_k^r(i)$ calculated from the a priori LLRs at the equalizer input. Notation " $s_k(i) : b_k^p(i)$ " represents the subset of symbols $s_k(i)$ in constellation \mathcal{A} with a given value (0 or 1) for $b_k^p(i)$.

III. METHOD FOR PREDICTING THE MULTI-USER TURBO-EQUALIZER/DEMAPPING PERFORMANCE

In this section, a simple method for predicting the performance of the multi-user turbo-equalization/demapping scheme will be developed.

The idea is to predict the behavior of the turbo-equalizer/demapper by solely looking separately at the input/output relations of each constituent stage (equalizer/demapper, decoder). More precisely, the mean and variance of the extrinsic LLRs output by each of the two stages will be determined as a function of the mean and the variance of their input LLRs, called a priori LLRs. This will be done in the two following subsections : subsection III-A will be devoted to the equalizer/demapper and subsection III-B to the decoder. Interleaver and de-interleaver do not of course affect those input/output relations. Gaussianity of the extrinsic LLRs output by the two stages will be assumed like in [4]. Its impact on the performance of our prediction method will be illustrated in section IV. Nevertheless, this Gaussian hypothesis is not needed for calculating the equalizer behavior as it will be explained later on in this section. It only reduces the number of equalizer input parameters to be considered (mean and variance of the distribution rather than the pdf itself). Both of the following subsections will successively consider single-user BPSK, single-user QPSK and multi-user BPSK cases. Both of them will also conclude with a few words on how to extend the methodology to high-order constellations.

A. Predicting the equalizer/demapper behavior

In the remainder of this paper, we will refer to the "equalizer/demapper" simply as the "equalizer" for the sake of conciseness. Before going through the different cases, let

$$g(x; \mu, \sigma^2) = \frac{1}{\sqrt{2\pi\sigma^2}} \exp \left(\frac{-(x-\mu)^2}{2\sigma^2} \right) \tag{12}$$

denote the pdf of a Gaussian random variable with mean μ and variance σ^2 . Let also

$$g_c(z; \mu, \sigma^2) = \frac{1}{\pi\sigma^2} \exp \left(\frac{-|z-\mu|^2}{\sigma^2} \right) \tag{13}$$

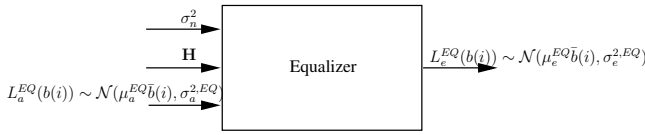


Fig. 3. Inputs and output of the equalizer. Single-user BPSK case.

denote the pdf of a complex Gaussian random variable, with mean μ and variance σ^2 , whose real and imaginary parts are independent and have the same variance $\sigma^2/2$. These notations will be often used in the sequel.

1) *Single-user BPSK case:* In the single-user BPSK case, $K = 1$, $q = 1$ and $M = 1$ (no spreading is needed). In the sequel we will thus leave out indexes k and p in all the notations introduced in section II. Defining $\bar{b}(i) \triangleq 2b(i) - 1$ ($\bar{b}(i) \in \{-1, 1\}$ and $b(i) \in \{0, 1\}$); for BPSK, $\bar{b}(i) = s(i)$, the a priori equalizer input LLRs $L_a^{EQ}(b(i))$ as well as the extrinsic equalizer output LLRs $L_e^{EQ}(b(i))$ on the interleaved coded bits $b(i)$ are assumed to be Gaussian distributed

$$L_a^{EQ}(b(i)) = \mu_a^{EQ} \bar{b}(i) + n_a^{EQ}(i), \quad (14)$$

$$L_e^{EQ}(b(i)) = \mu_e^{EQ} \bar{b}(i) + n_e^{EQ}(i), \quad (15)$$

with respective means μ_a^{EQ} and μ_e^{EQ} and respective variances $n_a^{EQ}(i) \sim \mathcal{N}(0, \sigma_a^{2, EQ})$ and $n_e^{EQ}(i) \sim \mathcal{N}(0, \sigma_e^{2, EQ})$.

As illustrated in Fig. 3, **the goal is to express the mean μ_e^{EQ} and the variance $\sigma_e^{2, EQ}$ of the extrinsic LLRs as functions of the mean μ_a^{EQ} and the variance $\sigma_a^{2, EQ}$ of the a priori LLRs as well as the noise variance σ_n^2 and the channel.** The reasoning will assume long frames and necessitate the calculation of an intermediary variable which will be named $\tilde{v}(\mu_a^{EQ}, \sigma_a^{2, EQ})$ hereafter.

It may be easily shown from the definition of LLR that $\tilde{s}(i) = \tanh(0.5 L_a^{EQ}(b(i)))$ and $\text{var}\{s(i)\} = 1 - \tanh^2(0.5 L_a^{EQ}(b(i)))$. Given this latter expression, (6) (leaving out index k) and (12), the mean of v calculated over the Gaussian distribution of the equalizer input LLRs may be expressed as (see appendix)

$$\tilde{v}(\mu_a^{EQ}, \sigma_a^{2, EQ}) = 1 - \int_{-\infty}^{+\infty} \tanh^2\left(\frac{y}{2}\right) g(y; \mu_a^{EQ}, \sigma_a^{2, EQ}) dy \quad (16)$$

where y is an integration variable. This integral may be computed numerically for any values of μ_a^{EQ} and $\sigma_a^{2, EQ}$. If the pdf of the equalizer a priori LLRs is known and may not be satisfactorily regarded as Gaussian, $\tilde{v}(\mu_a^{EQ}, \sigma_a^{2, EQ})$ may be calculated by incorporating this pdf in (16) rather than the Gaussian density.

Assuming long enough frames, the variance of v around its mean may be neglected. Indeed, v is then by (6) (without index k) the sum of a great number of random variables $\text{var}\{s(i)\}$ ($i = 1, \dots, I$) which may be assumed to be independent thanks to interleaving¹. Variable v may then be approximated by a deterministic value, namely its mean $\tilde{v}(\mu_a^{EQ}, \sigma_a^{2, EQ})$. Let now

¹ $\text{var}\{s(i)\} = 1 - \tanh^2(0.5 L_a^{EQ}(b(i)))$ are random variables since $L_a^{EQ}(b(i))$ are too.

$\tilde{\mathbf{R}}_{ss}$ denote matrix \mathbf{R}_{ss} when replacing v by $\tilde{v}(\mu_a^{EQ}, \sigma_a^{2, EQ})$, $\tilde{\mathbf{w}}$ denote vector \mathbf{w} when replacing \mathbf{R}_{ss} by $\tilde{\mathbf{R}}_{ss}$, $\tilde{\mu}$ and $\tilde{\sigma}_v^2$ respectively denote μ and σ_v^2 when replacing \mathbf{R}_{ss} and \mathbf{w} by $\tilde{\mathbf{R}}_{ss}$ and $\tilde{\mathbf{w}}$. Given $\hat{s}(i) = \mu s(i) + \nu(i)$, (10) - which gives

$$L_e^{EQ}(b(i)) = \frac{2\mu}{\sigma_v^2} \hat{s}(i) \quad (17)$$

in BPSK - and the previous definitions which consider μ and σ_v^2 as constants $\tilde{\mu}$ and $\tilde{\sigma}_v^2$, the mean and variance of the extrinsic LLRs output by the equalizer are given by

$$\begin{aligned} \mu_e^{EQ} &\triangleq E\{L_e^{EQ}(b(i)) | b(i) = 1\} \\ &= \frac{2\tilde{\mu}}{\tilde{\sigma}_v^2} E\{\hat{s}(i) | b(i) = s(i) = 1\} = \frac{2\tilde{\mu}^2}{\tilde{\sigma}_v^2}, \end{aligned} \quad (18)$$

$$\begin{aligned} \sigma_e^{2, EQ} &\triangleq \text{var}\{L_e^{EQ}(b(i))\} \\ &= \left(\frac{2\tilde{\mu}}{\tilde{\sigma}_v^2}\right)^2 \text{var}\{\hat{s}(i)\} = \frac{4\tilde{\mu}^2}{\tilde{\sigma}_v^2} = 2\mu_e^{EQ}. \end{aligned} \quad (19)$$

As $\tilde{\mu}$ and $\tilde{\sigma}_v^2$ depend on $\tilde{v}(\mu_a^{EQ}, \sigma_a^{2, EQ})$ and on σ_n^2 via $\tilde{\mathbf{w}}$, μ_e^{EQ} and $\sigma_e^{2, EQ}$ are functions of μ_a^{EQ} , $\sigma_a^{2, EQ}$ and σ_n^2 . The equalizer behavior may thus totally be predicted by the preceding calculations since we have expressed the mean and the variance of its output LLRs as functions of the mean and variance of its input LLRs, the noise variance and the channel matrix. The computational complexity of these calculations is very low since the sizes of vectors and matrices involved in calculations of μ_e^{EQ} and $\sigma_e^{2, EQ}$ are small and independent of the frame length.

2) *Single-user QPSK case:* In the single-user QPSK case, $K = 1$, $q = 2$ and $M = 1$ (no spreading is needed). In the sequel we will thus leave out indexes k in the notations but not index p which can take on values 1 or 2. Defining $\bar{b}^p(i) \triangleq 2b^p(i) - 1$ ($p = 1, 2$, $\bar{b}^p(i) \in \{-1, 1\}$ and $b^p(i) \in \{0, 1\}$), the a priori equalizer input LLRs $L_a^{EQ}(b^1(i))$ and $L_a^{EQ}(b^2(i))$ as well as the extrinsic equalizer output LLRs $L_e^{EQ}(b^1(i))$ and $L_e^{EQ}(b^2(i))$ on the interleaved coded bits $b^1(i)$ and $b^2(i)$ are assumed to be Gaussian distributed. Whereas it may be assumed that both $L_a^{EQ}(b^1(i))$ and $L_a^{EQ}(b^2(i))$ have the same mean and variance

$$L_a^{EQ}(b^p(i)) = \mu_a^{EQ} \bar{b}^p(i) + n_{a,p}^{EQ}(i) \quad p = 1, 2 \quad (20)$$

with $n_{a,p}^{EQ}(i) \sim \mathcal{N}(0, \sigma_a^{2, EQ})$, simulations reveal that $L_e^{EQ}(b^1(i))$ and $L_e^{EQ}(b^2(i))$ calculated from (10) have in general ² different means and variances

$$L_e^{EQ}(b^p(i)) = \mu_{e,p}^{EQ} \bar{b}^p(i) + n_{e,p}^{EQ}(i) \quad p = 1, 2$$

with $n_{e,p}^{EQ}(i) \sim \mathcal{N}(0, \sigma_{e,p}^{2, EQ})$. This will be intuitively explained in the appendix and illustrated in section IV.

As illustrated in Fig. 4, **the goal is to express the means $\mu_{e,1}^{EQ}$, $\mu_{e,2}^{EQ}$ and the variances $\sigma_{e,1}^{2, EQ}$, $\sigma_{e,2}^{2, EQ}$ of the extrinsic LLRs as functions of the mean μ_a^{EQ} and the variance $\sigma_a^{2, EQ}$ of the a priori LLRs as well as the noise variance σ_n^2 and the channel.** Exactly as for BPSK, the reasoning will assume long frames and necessitate the calculation of

²It depends on the choice of constellation mapping.

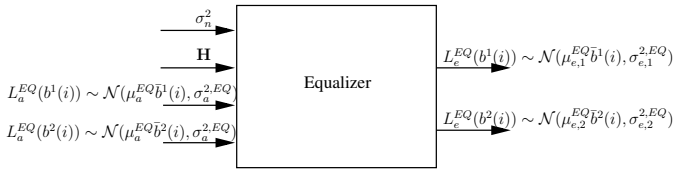


Fig. 4. Inputs and outputs of the equalizer. Single-user QPSK case.

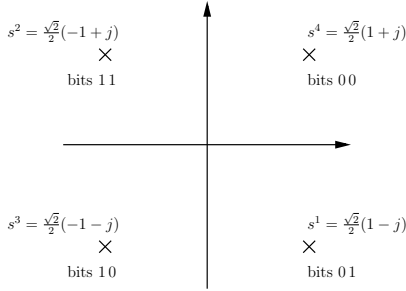


Fig. 5. Considered QPSK constellation.

an intermediary variable which will be named $\tilde{v}(\mu_a^{EQ}, \sigma_a^{2,EQ})$ hereafter.

Let us assume for the subsequent calculations that the four symbols of the QPSK constellation are chosen such that $s^1 = \frac{\sqrt{2}}{2}(1 - j)$, $s^2 = \frac{\sqrt{2}}{2}(-1 + j)$, $s^3 = \frac{\sqrt{2}}{2}(-1 - j)$ and $s^4 = \frac{\sqrt{2}}{2}(1 + j)$ resulting from the mapping of respectively bits 01, 11, 10 and 00 as shown in Fig. 5. This mapping has been preferred to Gray labeling which leads to poor performance in iterative receivers [13]. Moreover, it does not imply more difficult analytical derivations. Then, assuming independent bits $b^1(i)$ and $b^2(i)$ thanks to interleaving

$$\tilde{s}(i) =$$

$$\frac{1}{\left(e^{\frac{1}{2}L_a^{EQ}(b^1(i))} + e^{-\frac{1}{2}L_a^{EQ}(b^1(i))} \right) \left(e^{\frac{1}{2}L_a^{EQ}(b^2(i))} + e^{-\frac{1}{2}L_a^{EQ}(b^2(i))} \right)} \times \left[s^1 e^{\frac{1}{2}[L_a^{EQ}(b^1(i)) - L_a^{EQ}(b^2(i))]} + s^2 e^{\frac{1}{2}[L_a^{EQ}(b^1(i)) + L_a^{EQ}(b^2(i))]} + s^3 e^{\frac{1}{2}[-L_a^{EQ}(b^1(i)) + L_a^{EQ}(b^2(i))]} + s^4 e^{\frac{1}{2}[-L_a^{EQ}(b^1(i)) - L_a^{EQ}(b^2(i))]} \right] \quad (21)$$

Since $E\{|s(i)|^2\} = 1 \forall i$ for the considered QPSK constellation, $\text{var}\{s(i)\} = 1 - |\tilde{s}(i)|^2$. Given these two expressions, (6) (leaving out index k) and (12), the mean of v calculated over the Gaussian distribution of the equalizer input LLRs may be expressed as (see appendix)

$$\tilde{v}(\mu_a^{EQ}, \sigma_a^{2,EQ}) = 1 - \int_{-\infty}^{+\infty} \int_{-\infty}^{+\infty} \left[|\tilde{s}(i)|^2 \left| \frac{L_a^{EQ}(b^1(i))=y_1}{L_a^{EQ}(b^2(i))=y_2} \right| \right] \times g(y_1; \mu_a^{EQ}, \sigma_a^{2,EQ}) g(y_2; \mu_a^{EQ}, \sigma_a^{2,EQ}) dy_1 dy_2 \quad (22)$$

where y_1 and y_2 are integration variables. Notation $|\tilde{s}(i)|^2 \left| \frac{L_a^{EQ}(b^1(i))=y_1}{L_a^{EQ}(b^2(i))=y_2} \right|$ means the squared modulus of expression (21) where $L_a^{EQ}(b^1(i))$ and $L_a^{EQ}(b^2(i))$ are replaced respectively by y_1 and y_2 . This double integral may be computed numerically for any values of μ_a^{EQ} and $\sigma_a^{2,EQ}$.

Exactly as for single-user BPSK case, assuming long frames, we will approximate variable v by its mean $\tilde{v}(\mu_a^{EQ}, \sigma_a^{2,EQ})$. We are now able to calculate matrix $\tilde{\mathbf{R}}_{\text{SS}}$ when replacing v by $\tilde{v}(\mu_a^{EQ}, \sigma_a^{2,EQ})$ in matrix \mathbf{R}_{SS} , vector $\tilde{\mathbf{w}}$ by replacing \mathbf{R}_{SS} by $\tilde{\mathbf{R}}_{\text{SS}}$ in \mathbf{w} and eventually $\tilde{\mu}$ and $\tilde{\sigma}_v^2$ by replacing \mathbf{R}_{SS} and \mathbf{w} respectively by $\tilde{\mathbf{R}}_{\text{SS}}$ and $\tilde{\mathbf{w}}$ in the expressions of μ and σ_v^2 .

The only step remaining is the calculation of the means and variances of the extrinsic LLRs output by the equalizer. Given $\hat{s}(i) = \mu s(i) + \nu(i)$, (10), (12), (13) and the previous definitions which consider μ and σ_v^2 as constants $\tilde{\mu}$ and $\tilde{\sigma}_v^2$, $\mu_{e,1}^{EQ}$ and $\sigma_{e,1}^{2,EQ}$ are given by

$$\mu_{e,1}^{EQ} = E\{L_e^{EQ}(b^1(i)) | b^1(i) = 1\} = \int_{-\infty}^{+\infty} \int_{-\infty}^{+\infty} \int_{-\infty}^{+\infty} \left[L_e^{EQ}(b^1(i)) \left| \frac{\mu=\tilde{\mu}, \sigma_v^2=\tilde{\sigma}_v^2}{\hat{s}(i)=\hat{s}_p + j\hat{s}_q, L_a^{EQ}(b^2(i))=y_2} \right| \right] \left[\frac{1}{2} g_c(\hat{s}_p + j\hat{s}_q; \tilde{\mu} s^2, \tilde{\sigma}_v^2) g(y_2; \mu_a^{EQ}, \sigma_a^{2,EQ}) + \frac{1}{2} g_c(\hat{s}_p + j\hat{s}_q; \tilde{\mu} s^3, \tilde{\sigma}_v^2) g(y_2; -\mu_a^{EQ}, \sigma_a^{2,EQ}) \right] d\hat{s}_p d\hat{s}_q dy_2 \quad (23)$$

$$\sigma_{e,1}^{2,EQ} = E\{(L_e^{EQ}(b^1(i)))^2 | b^1(i) = 1\} - (\mu_{e,1}^{EQ})^2 = \int_{-\infty}^{+\infty} \int_{-\infty}^{+\infty} \int_{-\infty}^{+\infty} \left[(L_e^{EQ}(b^1(i)))^2 \left| \frac{\mu=\tilde{\mu}, \sigma_v^2=\tilde{\sigma}_v^2}{\hat{s}(i)=\hat{s}_p + j\hat{s}_q, L_a^{EQ}(b^2(i))=y_2} \right| \right] \left[\frac{1}{2} g_c(\hat{s}_p + j\hat{s}_q; \tilde{\mu} s^2, \tilde{\sigma}_v^2) g(y_2; \mu_a^{EQ}, \sigma_a^{2,EQ}) + \frac{1}{2} g_c(\hat{s}_p + j\hat{s}_q; \tilde{\mu} s^3, \tilde{\sigma}_v^2) g(y_2; -\mu_a^{EQ}, \sigma_a^{2,EQ}) \right] d\hat{s}_p d\hat{s}_q dy_2 - (\mu_{e,1}^{EQ})^2 \quad (24)$$

where \hat{s}_p , \hat{s}_q and y_2 are integration variables. Similar expressions for $\mu_{e,2}^{EQ}$ and $\sigma_{e,2}^{2,EQ}$ are given in appendix. As obtaining very accurate values of $\mu_{e,p}^{EQ}$ and $\sigma_{e,p}^{2,EQ}$ ($p = 1, 2$) turned out to be not necessary for the subsequent treatment by the decoder (a precision of 0.01 is more than enough), computation of the triple integrals in (23) and (24) is not too time prohibitive. Calculation of $\tilde{v}(\mu_a^{EQ}, \sigma_a^{2,EQ})$ in (22) is a bit more time-consuming. Indeed, more accuracy is needed for $\tilde{v}(\mu_a^{EQ}, \sigma_a^{2,EQ})$ since after being calculated this variable will intervene in expressions of $\mu_{e,1}^{EQ}$, $\mu_{e,2}^{EQ}$, $\sigma_{e,1}^{2,EQ}$ and $\sigma_{e,2}^{2,EQ}$.

It turns out thanks to simulations that $\sigma_{e,1}^{2,EQ} \cong 2\mu_{e,1}^{EQ}$ and $\sigma_{e,2}^{2,EQ} \cong 2\mu_{e,2}^{EQ}$. This may be justified using the consistency condition [12] for the LLR-value distribution.

As $\tilde{\mu}$ and $\tilde{\sigma}_v^2$ depend on $\tilde{v}(\mu_a^{EQ}, \sigma_a^{2,EQ})$ and on σ_n^2 via $\tilde{\mathbf{w}}$, $\mu_{e,1}^{EQ}$, $\sigma_{e,1}^{2,EQ}$, $\mu_{e,2}^{EQ}$, $\sigma_{e,2}^{2,EQ}$ are all functions of μ_a^{EQ} , $\sigma_a^{2,EQ}$ and σ_n^2 . Like in BPSK case, the equalizer behavior may thus totally be predicted by the preceding calculations since we have expressed the means and the variances of its output LLRs as functions of the mean and variance of its input LLRs, the noise variance and the channel matrix.

Exactly as in the BPSK case, if the pdf of the equalizer input LLRs is not Gaussian but is known, formulas (22), (23) and (24) may be re-calculated by incorporating this pdf rather

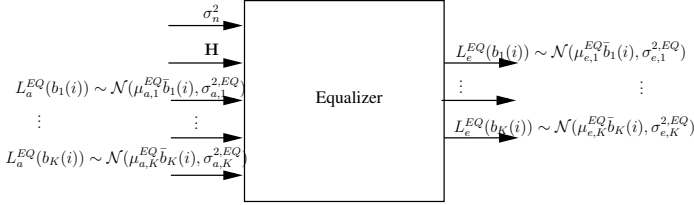


Fig. 6. Inputs and outputs of the equalizer. Multi-User BPSK case.

than the Gaussian density.

3) *Multi-User BPSK case:* In this case, $q = 1$, K and M are assumed to be given. Index p will be left out. Defining $\bar{b}_k(i) \triangleq 2b_k(i) - 1$ ($\bar{b}_k(i) \in \{-1, 1\}$ and $b_k(i) \in \{0, 1\}$); for BPSK, $\bar{b}_k(i) = s_k(i)$), the k -th user a priori equalizer input LLRs $L_a^{EQ}(b_k(i))$ as well as the extrinsic equalizer output LLRs $L_e^{EQ}(b_k(i))$ on the interleaved coded bits $b_k(i)$ are assumed to be Gaussian-like distributed

$$\begin{aligned} L_a^{EQ}(b_k(i)) &= \mu_{a,k}^{EQ} \bar{b}_k(i) + n_{a,k}^{EQ}(i) \quad k = 1, \dots, K, \\ L_e^{EQ}(b_k(i)) &= \mu_{e,k}^{EQ} \bar{b}_k(i) + n_{e,k}^{EQ}(i) \quad k = 1, \dots, K \end{aligned}$$

with $n_{a,k}^{EQ}(i) \sim \mathcal{N}(0, \sigma_{a,k}^{2, EQ})$ and $n_{e,k}^{EQ}(i) \sim \mathcal{N}(0, \sigma_{e,k}^{2, EQ})$.

As illustrated in Fig. 6, **the goal is to express for each user k the mean $\mu_{e,k}^{EQ}$ and the variance $\sigma_{e,k}^{2, EQ}$ of his extrinsic LLRs as functions of the means $\mu_{a,1}^{EQ}, \dots, \mu_{a,K}^{EQ}$ and the variances $\sigma_{a,1}^{2, EQ}, \dots, \sigma_{a,K}^{2, EQ}$ of the a priori LLRs of all users as well as the noise variance σ_n^2 and the channel matrix \mathbf{H} defined in (2).** Again, the procedure will include the calculation of an intermediary variable called $\tilde{v}_k(\mu_{a,k}^{EQ}, \sigma_{a,k}^{2, EQ})$.

Since $\tilde{s}_k(i) = \tanh(0.5 L_a^{EQ}(b_k(i)))$ and $\text{var}\{s_k(i)\} = 1 - \tanh^2(0.5 L_a^{EQ}(b_k(i)))$, the mean of v_k (defined in (6)) calculated over the Gaussian distribution of the k -th user equalizer input LLRs may be expressed similarly as in the single-user case by

$$\tilde{v}_k(\mu_{a,k}^{EQ}, \sigma_{a,k}^{2, EQ}) = 1 - \int_{-\infty}^{+\infty} \tanh^2\left(\frac{y}{2}\right) g(y; \mu_{a,k}^{EQ}, \sigma_{a,k}^{2, EQ}) dy. \quad (25)$$

This integral may be computed numerically for any values of $\mu_{a,k}^{EQ}$ and $\sigma_{a,k}^{2, EQ}$.

If we assume as usual long enough frames, the variance of v_k around its mean may be neglected. Then we approximate v_k ($\forall k = 1, \dots, K$) by a constant value, namely its mean $\tilde{v}_k(\mu_{a,k}^{EQ}, \sigma_{a,k}^{2, EQ})$. Let now $\tilde{\mathbf{R}}_{\text{ss},k}$ denote matrix $\mathbf{R}_{\text{ss},k}$ when replacing v_1 by $\tilde{v}_1(\mu_{a,1}^{EQ}, \sigma_{a,1}^{2, EQ}), \dots, v_K$ by $\tilde{v}_K(\mu_{a,K}^{EQ}, \sigma_{a,K}^{2, EQ})$, $\tilde{\mathbf{w}}_k$ denote vector \mathbf{w}_k when replacing $\mathbf{R}_{\text{ss},k}$ by $\tilde{\mathbf{R}}_{\text{ss},k}$, $\tilde{\mu}_k$ and $\tilde{\sigma}_{\nu_k}^2$ respectively denote μ_k and $\sigma_{\nu_k}^2$ when replacing $\mathbf{R}_{\text{ss},k}$ and \mathbf{w}_k by $\tilde{\mathbf{R}}_{\text{ss},k}$ and $\tilde{\mathbf{w}}_k$. Given (7), (10) - which gives

$$L_e^{EQ}(b_k(i)) = \frac{2\mu_k}{\sigma_{\nu_k}^2} s_k(i) \quad (26)$$

in multiuser BPSK - and the previous definitions which consider μ_k and $\sigma_{\nu_k}^2$ as constants $\tilde{\mu}_k$ and $\tilde{\sigma}_{\nu_k}^2$, the mean and variance of the k -th user ($k = 1, \dots, K$) extrinsic LLRs output

by the equalizer are given by

$$\mu_{e,k}^{EQ} \triangleq E\{L_e^{EQ}(b_k(i)) | b_k(i) = 1\} = \frac{2\tilde{\mu}_k^2}{\tilde{\sigma}_{\nu_k}^2} \quad (27)$$

$$\sigma_{e,k}^{2, EQ} \triangleq \text{var}\{L_e^{EQ}(b_k(i))\} = \frac{4\tilde{\mu}_k^2}{\tilde{\sigma}_{\nu_k}^2} = 2\mu_{e,k}^{EQ} \quad (28)$$

As, for each user k , $\tilde{\mu}_k$ and $\tilde{\sigma}_{\nu_k}^2$ depend on *all* $\mu_{a,k}^{EQ}$ and $\sigma_{a,k}^{2, EQ}$ ($\forall k = 1, \dots, K$) and on σ_n^2 via $\tilde{\mathbf{w}}_k$, $\mu_{e,k}^{EQ}$ and $\sigma_{e,k}^{2, EQ}$ are functions of $\mu_{a,1}^{EQ}, \dots, \mu_{a,K}^{EQ}$, $\sigma_{a,1}^{2, EQ}, \dots, \sigma_{a,K}^{2, EQ}$ and σ_n^2 . Consequently, we succeeded in expressing for each user the mean and the variance of his extrinsic LLRs as functions of the means and the variances of the a priori LLRs of *all* users as well as the noise variance and the channel matrix.

4) *Generalization to higher-order constellations:* For single-user case with constellations with $q \geq 3$, the calculation of $|\tilde{s}(i)|^2$ needed for $\tilde{v}(\mu_a^{EQ}, \sigma_a^{2, EQ})$ requires a q -dimension integration. Moreover, for QAM constellations, $E\{|s(i)|^2\}$ is generally not equal to 1 and needs to be calculated by averaging on the equalizer input LLRs distribution. The expressions of the means and the variances of the q extrinsic LLRs output by the equalizer demand the calculation of a $(q+1)$ -dimension integral. Extension to the multi-user case with $q \geq 2$ may be performed by mixing the previous considerations with the methodology exposed in III-A.3.

B. Predicting the decoder behavior

1) *Single-user BPSK case:* Unlike the equalizer, the decoder behavior may only be predicted by simulations. However, in the single-user BPSK case, these simulations are not too time demanding since they let vary only one parameter at the decoder input : the mean of its a priori LLRs which is assumed to be Gaussian distributed. Indeed, the a priori decoder input LLRs are the de-interleaved extrinsic LLRs output by the equalizer. As we may see from (18) and (19), the mean and the variance of these LLRs are not independent since $\sigma_e^{2, EQ} = 2\mu_e^{EQ}$. Simulations of the decoder behavior may thus be performed by letting vary with a certain step the mean of its input LLRs from 0 up to a value regarded as great enough. For each of these simulated values, the mean and the variance of the extrinsic LLRs output by the decoder are stored in a look-up table. As we are interested in the system performance, the output BER corresponding to each simulated value is also retained.

2) *Single-user QPSK case:* The a priori decoder input LLRs are the de-interleaved equalizer extrinsic LLRs and the equalization stage outputs two independent parameters as explained in subsection III-A.2 : the means of its extrinsic LLRs $\mu_{e,1}^{EQ}$ and $\mu_{e,2}^{EQ}$ related to coded bits $b^1(i)$ and $b^2(i)$ since we assume $\sigma_{e,1}^{2, EQ} \cong 2\mu_{e,1}^{EQ}$ and $\sigma_{e,2}^{2, EQ} \cong 2\mu_{e,2}^{EQ}$. In practice, if running in advance simulations of the decoder for all possible values of the two input parameters is regarded as unaffordable, ordinary simulations are then still necessary. Nevertheless, thanks to the calculations made for the equalizer in subsection III-A the decoder will be the only block of the

whole communication chain which needs to be simulated. In other words, the performance of the system will be predictable by only simulating the decoder behavior.

3) *Multi-User BPSK case:* In the multi-user case, there are K decoders in the receiver block, each of them corresponding to one user. The K extrinsic LLRs $L_e^{EQ}(b_k(i))$ ($k = 1, \dots, K$) are split between the K decoders so that only one LLR head towards each decoder after deinterleaving. If using the same code for each user, simulations must be performed only once (and not K times). Moreover, since $\sigma_{e,k}^{2,EQ} = 2\mu_{e,k}^{EQ} \forall k$, they let vary only one parameter : the mean of the decoder input LLR. Exactly as in the single-user BPSK case, for each of these simulated values of this parameter, the mean and the variance of the extrinsic LLRs output by the decoder as well as the BER may be stored in a look-up table.

4) *Generalization to higher-order constellations:* The a priori decoder input LLRs are always the de-interleaved extrinsic LLRs output by the equalizer. For the single-user case, as explained in subsection III-A.4, the equalization stage outputs a number of independent parameters equal to the constellation order q . These are the means $\mu_{e,p}^{EQ}$ ($p = 1, \dots, q$) of the extrinsic LLRs output by the equalizer $L_e^{EQ}(b^p(i))$. Simulating in advance the decoder would then require to let vary q parameters at its input and store the decoder outputs for all possible values of these q input parameters. It is often unaffordable in practice. Real-time simulations are still needed but, like in the single-user QPSK case, the calculations made for the equalizer enable to reduce the simulation of the whole communication chain to that of the decoder only.

Extension to the multi-user case with $q \geq 2$ may be performed by mixing the previous considerations with those exposed in III-B.3.

C. Conclusion

In the case where the decoder is simulated in advance for all possible values of its input parameters, each constituent stage (equalizer, decoder) may thus be characterized by its input/output relations (calculated for the equalizer and simulated for the decoder). The overall system performance and convergence behavior may then be easily predicted at any iteration. Indeed, starting from null a priori equalizer LLRs at the first iteration, we may then proceed step by step by calculating (for the equalizer) or picking (for the decoder) the output parameters as functions of the inputs. Once the decoder has been simulated for some fixed parameters of the code (code rate, constraint length, ...), performance of the equalized system may be predicted given that decoder without further simulations for any frequency selective channels. System performance with the AWGN channel may also be obtained (case when $h_0 = 1$ and $h_j = 0 \forall j \neq 0$) as well as performance with perfect a priori information at the equalizer input. For this latter case, $\text{var}\{s_k(i)\}$ and $\tilde{v}(\mu_a^{EQ}, \sigma_a^{2,EQ})$ just need to be replaced by 0 everywhere in the previous equations since $\tilde{s}_k(i)$ then tends to $s_k(i)$ and $|s_k(i)|^2$ tends to 1 $\forall k, i$ with a normalized-to-unity constellation.

In the case where simulating the decoder in advance is too time prohibitive, as already said in subsection III-B, real-time simulations are still needed. However, the calculations made for the equalizer enable to reduce the simulation of the whole communication chain to that of the decoder only. The performance and convergence of the system is then predictable by only simulating the decoder behavior.

The efficiency of this prediction method will be illustrated in next section.

IV. RESULTS

We consider a rate-1/2 convolutional encoder with constraint length $K = 3$ and generator polynomials $[5_8, 7_8]$. Decoding is performed with well-known BCJR algorithm. In the sequel we consider length-11 Proakis A channel $[0.04, -0.05, 0.07, -0.21, -0.5, 0.72, 0.36, 0.0, 0.21, 0.03, 0.07]$ and length-5 Porat channel $[2-0.4j, 1.5+1.8j, 1, 1.2-1.3j, 0.8+1.6j]$. Both of them have to be normalized. We will present in subsections IV-A, IV-B and IV-C some results obtained respectively in the single-user BPSK case, in the single-user QPSK case and in the 8-PSK single-user case.

A. Single-user BPSK case

Simulations have been run for frames of 1024 BPSK coded symbols and 6 turbo iterations. The next two paragraphs will compare the results obtained with pure simulations and with our prediction method, respectively in terms of BER and in terms of numerical values for μ_a^{EQ} , $\sigma_a^{2,EQ}$, μ_e^{EQ} , $\sigma_e^{2,EQ}$. Each of the last two paragraphs of this subsection will present a graphical tool for studying the convergence of the turbo-equalizer. The first tool will explicitly emphasize the impact of the Gaussian approximation of the LLRs at the decoder output. The second one is the well-known EXIT chart.

Fig. 7 shows for iterations 1 and 2 the BER versus E_b/N_0 obtained with Proakis A channel, $N_1 = 0$ and $N_2 = 10$. For each simulated E_b/N_0 , 320 frame errors have been waited for. Figure 8 gives for iterations 1, 2 and 6 the performance obtained with Porat channel, $N_1 = 3$ and $N_2 = 7$. In each figure the solid curves represent the results obtained with plain simulations of the turbo equalization chain whereas the dashed curves are for results obtained with the proposed prediction method. The dashed bold curves with circles show the AWGN channel case or equivalently the perfect equalizer a priori information case. In this AWGN case, the curve obtained with pure simulations turned out to be indiscernible from that resulting from the application of the proposed method. In both figures solid and dashed curves are very close to each other and even tend to be indistinguishable which proves the efficiency of the prediction method.

Table I compares with numbers instead of graphics the values of μ_a^{EQ} , $\sigma_a^{2,EQ}$, μ_e^{EQ} , $\sigma_e^{2,EQ}$ and BER obtained with plain simulations ("Simulated equalizer") and with the prediction method ("Calculated equalizer") for the Porat channel. The data are given for the first four iterations and for $E_b/N_0 = 3.5$ dB. The closeness of the results in the two cases ("Simulated equalizer" and "Calculated equalizer") is again observed and also appears for other values of E_b/N_0 .

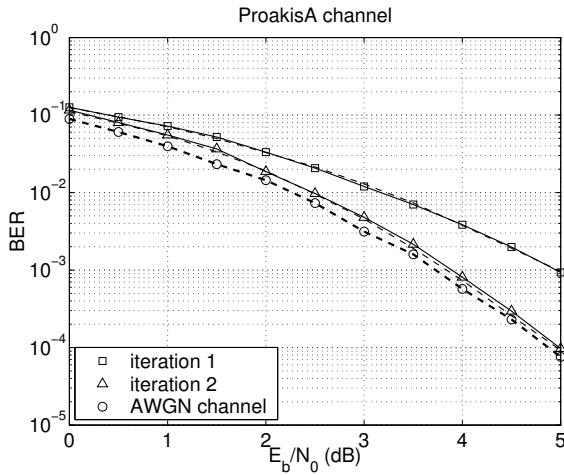


Fig. 7. Single-user BPSK case. Proakis A channel. Comparison between results obtained at iterations 1 and 2 with plain simulations (solid lines) and with prediction method (dotted lines).

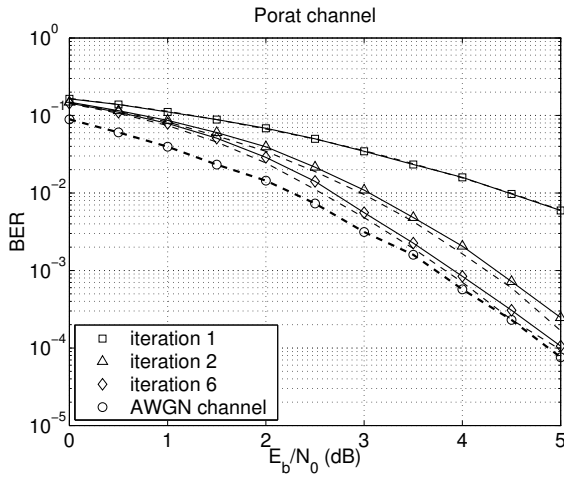


Fig. 8. Single-user BPSK case. Porat channel. Comparison between results obtained at iterations 1, 2 and 6 with plain simulations (solid lines) and with prediction method (dotted lines).

A first graphical tool for studying the convergence of the turbo-equalization scheme in the single-user BPSK case is now presented. As opposed to the EXIT chart in [4], the assumption $\sigma_a^{2,EQ} = 2\mu_a^{EQ}$ is not necessary. For that matter, it is not exactly the case in practice as it may be observed e.g. in Table I. Fig. 9 is for the Proakis A channel and Fig. 10 is for the Porat channel. Moreover, unlike the EXIT chart in [4], this tool is able to explicitly highlight the impact of the Gaussian approximation of the LLRs at the decoder output, as we will see hereafter. The x -axis represents the variable $1 - \tilde{v}(\mu_a^{EQ}, \sigma_a^{2,EQ})$ ($\tilde{v}(\mu_a^{EQ}, \sigma_a^{2,EQ})$ is simply denoted \tilde{v} in the sequel) of (6), the left y -axis the variable μ_e^{EQ} of (18) and the right y -axis the BER at the decoder output obtained for each value μ_e^{EQ} , itself proceeding from a corresponding $1 - \tilde{v}$ on the x -axis. In each of these figures, the dashed curve (“Decoder - Gaussian LLR”) represents the decoder characteristic assuming that the extrinsic LLRs output by the decoder are Gaussian-like distributed. It may be drawn in the following

TABLE I
SINGLE-USER BPSK CASE. $E_b/N_0 = 3.5\text{dB}$. PORAT CHANNEL.
COMPARISON OF PERFORMANCE WITH SIMULATED AND CALCULATED
EQUALIZERS.

Simulated equalizer					
Iteration	μ_a^{EQ}	$\sigma_a^{2,EQ}$	μ_e^{EQ}	$\sigma_e^{2,EQ}$	BER
1	0.0	0.0	2.84	5.66	$2.3 \cdot 10^{-2}$
2	4.96	11.02	3.84	7.65	$4.8 \cdot 10^{-3}$
3	8.88	17.15	4.24	8.47	$2.6 \cdot 10^{-3}$
4	10.46	19.35	4.33	8.66	$2.3 \cdot 10^{-3}$
5	10.80	19.79	4.34	8.69	$2.3 \cdot 10^{-3}$
6	10.86	19.88	4.34	8.70	$2.3 \cdot 10^{-3}$

Calculated equalizer					
Iteration	μ_a^{EQ}	$\sigma_a^{2,EQ}$	μ_e^{EQ}	$\sigma_e^{2,EQ}$	BER
1	0.0	0.0	2.84	5.68	$2.4 \cdot 10^{-2}$
2	4.94	11.14	3.86	7.72	$4.3 \cdot 10^{-3}$
3	8.94	17.45	4.26	8.52	$2.2 \cdot 10^{-3}$
4	10.54	19.59	4.34	8.69	$1.9 \cdot 10^{-3}$
5	10.84	20.11	4.36	8.71	$1.9 \cdot 10^{-3}$
6	10.94	20.20	4.36	8.72	$1.9 \cdot 10^{-3}$

way. As explained in subsection III-B.1, μ_a^{EQ} and $\sigma_a^{2,EQ}$ may be obtained from μ_e^{EQ} by decoder *simulations*. Then \tilde{v} may be computed by (16). The solid curves with the squares, triangles and circles are the equalizer characteristics respectively for E_b/N_0 equal to 0dB, 3dB and 5dB. They may be *calculated* from \tilde{v} as explained in subsection III-A.2. Exactly like in EXIT charts [6], the system convergence behavior may be visualized as a zigzagging trajectory between the equalizer and decoder characteristics. For each E_b/N_0 , the intersection of these two curves gives the final convergence point which may be reached by the turbo-equalization scheme. The solid curve (“Decoder - True LLR”) represents the decoder characteristic when \tilde{v} is calculated from the actual distribution of the decoder extrinsic LLRs (i.e. gaussianity of these LLRs is no longer assumed). The gap between the decoder solid and dotted curves gives thus the impact on the prediction method when considering that those decoder extrinsic LLRs are Gaussian-like distributed. This impact appears to be very limited as we could already notice it in Fig. 7, Fig. 8 and Table I (the performance with the calculated equalizer - which assumed gaussianity of the LLRs - was seen to be little different from that with the actual equalizer). As the decoder dashed curve is slightly under the solid curve for any $\tilde{v} \in [0, 1]$, the prediction method tends to over-estimate the system performance which is confirmed in Fig. 7 and 8. In Fig. 9 and 10 which only differ by the channel, the curves related to the decoder and the BER are of course the same. Notice that the decoder characteristic curve (not represented in Fig. 9 and 10 for the sake of clarity) assuming $\sigma_a^{2,EQ} = 2\mu_a^{EQ}$ would be here very close to the decoder solid and dashed curves. Assuming $\sigma_a^{2,EQ} = 2\mu_a^{EQ}$ like in [4] would thus not deteriorate the prediction method with the chosen convolutional decoder.

Consequently, as explained in [4], an EXIT chart may be drawn to study the system convergence behavior. It shows the evolution throughout the iterations of the mutual information

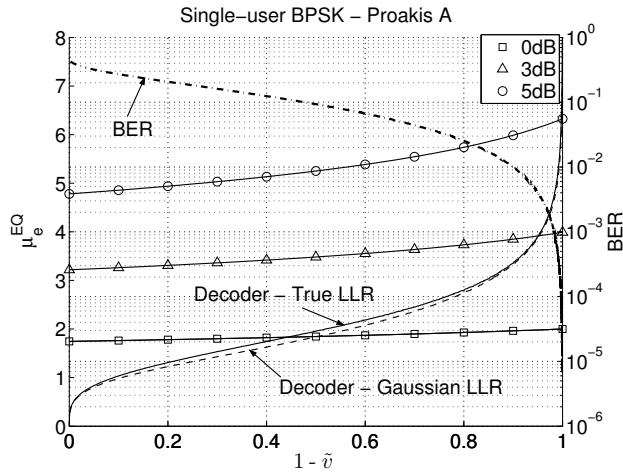


Fig. 9. Single-user BPSK case. Proakis A channel. Convergence graphical tool. Illustration of the impact of the Gaussian approximation of the LLRs at the decoder output.

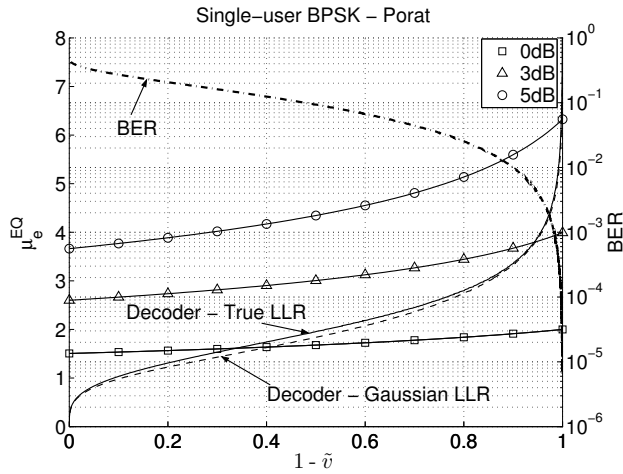


Fig. 10. Single-user BPSK case. Porat channel. Convergence graphical tool. Illustration of the impact of the Gaussian approximation of the LLRs at the decoder output.

between the equalizer and decoder input LLRs and the actual transmitted bits. Such an EXIT chart is given in Fig. 11 for the Porat channel and the chosen convolutional code. On the x -axis, I_a equalizer (I_e decoder) is the mutual information at the equalizer input (or equivalently at the decoder output). On the y -axis, I_e equalizer (I_a decoder) is the mutual information at the equalizer output (or equivalently at the decoder input). Unlike the decoder curve which has been simulated (solid line in Fig. 11), the equalizer curves have been *calculated* (such curves were simulated in [4]) for $E_b/N_0 = 0\text{dB}$, 3dB and 5dB thanks to the prediction method described in subsection III-A. Dotted lines show the actual evolution of the mutual information throughout the iterations when pure simulations of the turbo-equalizer are performed. As the dotted lines trajectories almost remain on the equalizer and decoder characteristic curves, the efficiency of the prediction method is once again illustrated. Let us remind that there is a one-to-one mapping between the mean μ of a LLR distribution (or

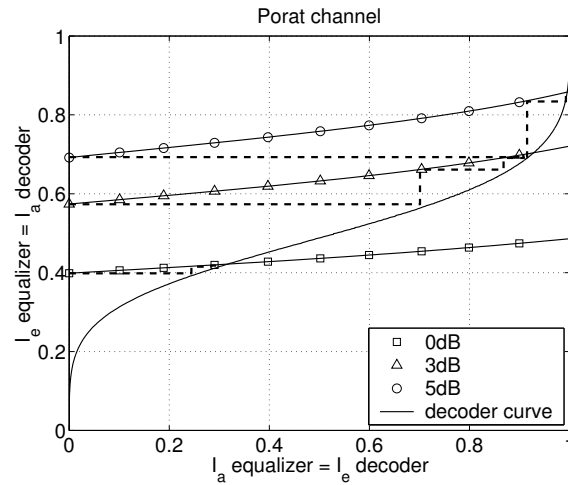


Fig. 11. Single-user BPSK case. Porat channel. Exit chart at $E_b/N_0 = 0\text{dB}$, 3dB , 5dB . The equalizer curves have been calculated. The dotted lines show the actual evolution of the mutual information throughout the iterations when pure simulations are performed.

equivalently its variance σ^2 since we assume here $\mu = \frac{1}{2}\sigma^2$) and the mutual information I between this distribution and the actual symbols. It is clearly explained in [6]. So Fig. 11 could also have been drawn with μ_e^{EQ} on the y -axis and μ_a^{EQ} on the x -axis.

B. Single-user QPSK case

Let us now consider the single-user QPSK case. Simulations have now been run for frames of 3072 QPSK symbols.

Fig. 12 shows for iterations 1, 3, 5 and 8 the BER versus E_b/N_0 obtained with Porat channel ($N_1 = 3$ and $N_2 = 7$). For each simulated E_b/N_0 , 320 frame errors have again been waited for. As for BPSK case, the solid curves represent the results obtained with plain simulations of the turbo-equalization scheme whereas the dashed curves are for results obtained with the proposed prediction method. In this latter case, as explained in subsection III-B.2, decoder simulations were not run in advance unlike the BPSK case but were performed in real time, here even without assuming that $\sigma_{e,1}^{2,EQ} = 2\mu_{e,1}^{EQ}$ and $\sigma_{e,2}^{2,EQ} = 2\mu_{e,2}^{EQ}$. Solid and dashed curves almost perfectly overlap, which proves again the efficiency of the prediction method. The little gap between the solid and dashed curves gives the slight impact on the performance prediction when assuming gaussianity of the LLRs output by the equalizer and the decoder.

Fig. 13 shows for the Porat channel and mapping of Fig. 5 the distribution (pdf) of LLRs $L_e^{EQ}(b^1(i))$ and $L_e^{EQ}(b^2(i))$ at the equalizer output at $E_b/N_0 = 3.5\text{dB}$ and at 4th iteration. Solid lines (barely visible because nearly indistinguishable from dotted lines) show the actual pdfs of these LLRs obtained by pure simulations. Dotted lines represent the Gaussian densities which have the same mean and variance as the actual distributions. We clearly notice that $L_e^{EQ}(b^1(i))$ and $L_e^{EQ}(b^2(i))$ may be both very good approximated by Gaussian densities, each of them with specific mean and variance. The global LLR distribution at the equalizer output is thus

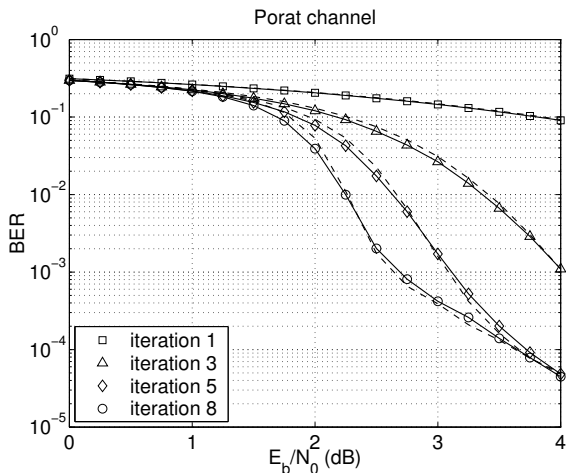


Fig. 12. Single-user QPSK case. Porat channel. Comparison between results obtained at iterations 1, 3, 5 and 8 with plain simulations (solid lines) and with prediction method (dotted lines).

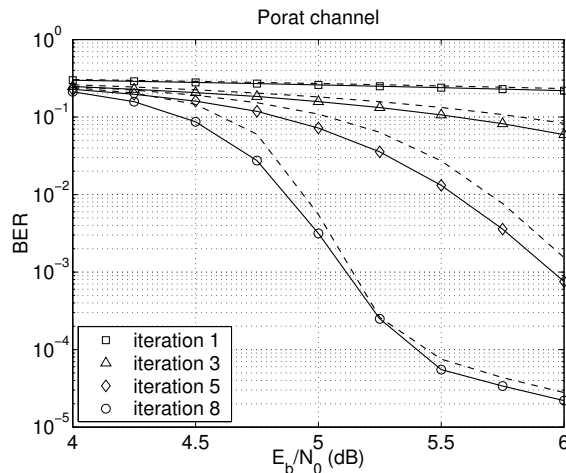


Fig. 14. Single-user 8-PSK case. Porat channel. Comparison between results obtained at iterations 1, 3, 5 and 8 with plain simulations (solid lines) and with prediction method (dotted lines).

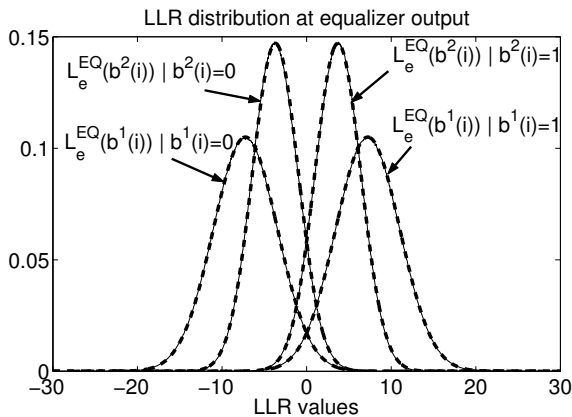


Fig. 13. Single-user QPSK case. Mapping given in Fig. 5. Porat channel. Distribution of LLRs at the equalizer output at $E_b/N_0 = 3.5\text{dB}$ and at 4th iteration.

a mixture of two Gaussian probability densities, each of them corresponding to one bit ($b^1(i)$ or $b^2(i)$) of the QPSK symbol. It is also the case for other values of E_b/N_0 and other iterations. In general, this Gaussian mixture cannot be satisfactorily reduced to only one equivalent Gaussian density. Moreover, it may be proved that this mixture depends on the particular choice of constellation mapping. For example, with QPSK Gray mapping, the distributions of $L_e^{EQ}(b^1(i))$ and $L_e^{EQ}(b^2(i))$ - which may also be good approximated by Gaussian densities (not illustrated in this paper) - do perfectly overlap ($\mu_{e,1}^{EQ} = \mu_{e,2}^{EQ}$ and $\sigma_{e,1}^{2,EQ} = \sigma_{e,2}^{2,EQ}$).

C. Single-user 8-PSK case

Let us conclude this section with the single-user 8-PSK case. The 8 symbols of the constellation have been chosen as follows : $s^1 = 1$, $s^2 = \frac{\sqrt{2}}{2}(1 + j)$, $s^3 = j$, $s^4 = \frac{\sqrt{2}}{2}(-1 + j)$, $s^5 = -1$, $s^6 = \frac{\sqrt{2}}{2}(-1 - j)$, $s^7 = -j$ and $s^8 = \frac{\sqrt{2}}{2}(1 - j)$ resulting from the mapping of respectively bits 000, 100, 010, 110, 001, 101, 011 and 111. Simulations have now been run for frames of 6144 8-PSK symbols.

V. CONCLUSION

This paper proposes a simple semi-analytical method with reduced simulation time to predict at any iteration the performance of a turbo-equalization/demapping scheme using the Wang and Poor soft-in/soft-out (SISO) Minimum Mean Square Error (MMSE) / Interference Cancellation (IC) equalizer and a SISO decoder. The proposed method may be applied to multi-level/phase data modulations as well as multi-user contexts. Gaussianity of the extrinsic Log-Likelihood Ratios (LLRs) output by the equalizer as well as the decoder is assumed and the impact of this hypothesis on the performance prediction has been illustrated.

This paper shows that the equalizer behavior may be very reliably predicted totally by calculations (no simulations are needed) whereas that of the decoder still requires simulations. Comparison between the proposed prediction method and plain simulations of the overall turbo equalization scheme demonstrates that our method accurately determines the system performance at any iteration.

The developed prediction method also significantly reduces the number of simulations needed to draw the EXIT chart in the single-user BPSK case.

APPENDIX

This appendix gives additional formulas for subsection III-A.

1) *Single-user BPSK*: The calculation of $\tilde{\nu}(\mu_a^{EQ}, \sigma_a^{2,EQ})$ in this case is actually obtained by averaging $\text{var}\{s(i)\} = 1 - \tanh^2(0.5 L_a^{EQ}(b(i)))$ over the assumed Gaussian distribution

of the LLRs at the equalizer input (see (14)) :

$$\tilde{v}(\mu_a^{EQ}, \sigma_a^{2, EQ}) = 1 - \int_{-\infty}^{+\infty} \tanh^2\left(\frac{y}{2}\right) \times \left(\frac{1}{2} g(y; \mu_a^{EQ}, \sigma_a^{2, EQ}) + \frac{1}{2} g(y; -\mu_a^{EQ}, \sigma_a^{2, EQ}) \right) dy$$

where the two terms in the integral accounts respectively for the two equally likely possibilities $s(i) = +1$ and $s(i) = -1$. It may be easily shown that the contribution of these two terms to the integral is identical. So $\tilde{v}(\mu_a^{EQ}, \sigma_a^{2, EQ})$ is simply given by (16).

2) *Single-user QPSK*: The calculation of $\tilde{v}(\mu_a^{EQ}, \sigma_a^{2, EQ})$ is obtained, like in BPSK, by averaging $\text{var}\{s(i)\} = 1 - E\{|\tilde{s}(i)|^2\}$ over the assumed Gaussian distribution of the LLRs at the equalizer input (see (20)) :

$$\tilde{v}(\mu_a^{EQ}, \sigma_a^{2, EQ}) = 1 - \int_{-\infty}^{+\infty} \int_{-\infty}^{+\infty} \left[|\tilde{s}(i)|^2 \Big|_{\substack{L_a^{EQ}(b^1(i))=y_1 \\ L_a^{EQ}(b^2(i))=y_2}} \right] \times \left[\frac{1}{4} g(y_1; -\mu_a^{EQ}, \sigma_a^{2, EQ}) g(y_2; \mu_a^{EQ}, \sigma_a^{2, EQ}) + \frac{1}{4} g(y_1; \mu_a^{EQ}, \sigma_a^{2, EQ}) g(y_2; \mu_a^{EQ}, \sigma_a^{2, EQ}) + \frac{1}{4} g(y_1; \mu_a^{EQ}, \sigma_a^{2, EQ}) g(y_2; -\mu_a^{EQ}, \sigma_a^{2, EQ}) + \frac{1}{4} g(y_1; -\mu_a^{EQ}, \sigma_a^{2, EQ}) g(y_2; -\mu_a^{EQ}, \sigma_a^{2, EQ}) \right] dy_1 dy_2$$

where the terms in the integral accounts respectively for the four equiprobable possibilities $s(i) = s^1$, $s(i) = s^2$, $s(i) = s^3$, $s(i) = s^4$ and notation $|\tilde{s}(i)|^2 \Big|_{\substack{L_a^{EQ}(b^1(i))=y_1 \\ L_a^{EQ}(b^2(i))=y_2}}$ means the squared modulus of expression (21) where $L_a^{EQ}(b^1(i))$ and $L_a^{EQ}(b^2(i))$ are replaced respectively by y_1 and y_2 . Due to the $\pi/2$ rotational symmetry of the considered constellation, the contribution of these four terms to the integral is identical and $\tilde{v}(\mu_a^{EQ}, \sigma_a^{2, EQ})$ is simply given by (22).

Whereas the mean and the variance of the equalizer extrinsic LLRs related to the first bit of symbol $s(i)$ are given by (23) and (24), those concerning the second bit may be calculated as

$$\mu_{e,2}^{EQ} = E\{L_e^{EQ}(b^2(i)) | b^2(i) = 1\} = \int_{-\infty}^{+\infty} \int_{-\infty}^{+\infty} \int_{-\infty}^{+\infty} \left[L_e^{EQ}(b^2(i)) \Big|_{\substack{\mu=\tilde{\mu}, \sigma_\nu^2=\tilde{\sigma}_\nu^2 \\ \hat{s}(i)=\hat{s}_p+j\hat{s}_q, L_a^{EQ}(b^1(i))=y_1}} \right] \left[\frac{1}{2} g_c(\hat{s}_p + j\hat{s}_q; \tilde{\mu} s^1, \tilde{\sigma}_\nu^2) g(y_1; -\mu_a^{EQ}, \sigma_a^{2, EQ}) + \frac{1}{2} g_c(\hat{s}_p + j\hat{s}_q; \tilde{\mu} s^2, \tilde{\sigma}_\nu^2) g(y_1; \mu_a^{EQ}, \sigma_a^{2, EQ}) \right] d\hat{s}_p d\hat{s}_q dy_1$$

$$\sigma_{e,2}^{2, EQ} = E\{(L_e^{EQ}(b^2(i)))^2 | b^2(i) = 1\} - \left(\mu_{e,2}^{EQ}\right)^2 = \int_{-\infty}^{+\infty} \int_{-\infty}^{+\infty} \int_{-\infty}^{+\infty} \left[(L_e^{EQ}(b^2(i)))^2 \Big|_{\substack{\mu=\tilde{\mu}, \sigma_\nu^2=\tilde{\sigma}_\nu^2 \\ \hat{s}(i)=\hat{s}_p+j\hat{s}_q, L_a^{EQ}(b^1(i))=y_1}} \right] \left[\frac{1}{2} g_c(\hat{s}_p + j\hat{s}_q; \tilde{\mu} s^1, \tilde{\sigma}_\nu^2) g(y_1; -\mu_a^{EQ}, \sigma_a^{2, EQ}) + \frac{1}{2} g_c(\hat{s}_p + j\hat{s}_q; \tilde{\mu} s^2, \tilde{\sigma}_\nu^2) g(y_1; \mu_a^{EQ}, \sigma_a^{2, EQ}) \right] d\hat{s}_p d\hat{s}_q dy_1 - \left(\mu_{e,2}^{EQ}\right)^2$$

Let us now explain why in general $\mu_{e,1}^{EQ} \neq \mu_{e,2}^{EQ}$ and $\sigma_{e,1}^{2, EQ} \neq \sigma_{e,2}^{2, EQ}$. Considering the constellation mapping of Fig. 5, we may notice that a good knowledge (brought by a large value of its related LLR) on the second bit $b^2(i)$ of a QPSK symbol enables to hesitate between symbols s^1 and s^2 (if we are quite sure that $b^2(i) = 1$) or between symbols s^3 and s^4 (if we are quite sure that $b^2(i) = 0$). Symbols s^1 and s^2 are precisely quite distant in the constellation (their distance is the diagonal length of the constellation square). So are s^1 and s^2 . Thus a good knowledge of $b^2(i)$, i.e. a large value of LLR $L_e^{EQ}(b^2(i))$, brings an even better knowledge of $b^1(i)$, i.e. an even greater absolute value of LLR $L_e^{EQ}(b^1(i))$.

REFERENCES

- [1] A. Dejonghe and L. Vandendorpe, "Turbo-equalization for multilevel modulation : an efficient low-complexity scheme," in *IEEE International Conference on Communications, ICC*, New York, USA, May 2002, vol. 3, pp. 1863–1867.
- [2] X. Wang and V. Poor, "Iterative (turbo) soft interference cancellation and decoding for coded CDMA," *IEEE Transactions on Communications*, vol. 47, pp. 1046–1061, July 1999.
- [3] X. Wautelet, A. Dejonghe, and L. Vandendorpe, "MMSE-based fractional turbo receiver for space-time BICM over frequency-selective MIMO fading channels," *IEEE Transactions on Signal Processing*, vol. 52, pp. 1804–1809, June 2004.
- [4] M. Tüchler, R. Koetter, and A.C. Singer, "Turbo equalization : principles and new results," *IEEE Transactions on Communications*, vol. 50, no. 5, pp. 754–767, May 2002.
- [5] L.R. Bahl and al., "Optimal decoding of linear codes for minimizing symbol error rate," *IEEE Transactions on Information Theory*, pp. 284–287, 1974.
- [6] S. Ten Brink, "Convergence behavior of iteratively decoded parallel concatenated codes," *IEEE Transactions on Communications*, vol. 49, no. 10, pp. 1727–1737, Oct. 2001.
- [7] M. Fu, "Stochastic analysis of turbo decoding," *IEEE Transactions on Information Theory*, vol. 51, no. 1, pp. 81–100, Jan. 2005.
- [8] P.D. Alexander, A.J. Grant, and M.C. Reed, "Iterative detection on code-division multiple-access with error control coding," *European Transactions on Telecommunications*, vol. 9, no. 5, pp. 419–426, Oct. 1998.
- [9] K.R. Narayanan, X. Wang, and G. Yue, "Estimating the PDF of the SIC-MMSE equalizer output and its applications in designing LDPC codes with turbo equalization," *IEEE Transactions on Wireless Communications*, vol. 4, no. 1, pp. 278–287, Jan. 2005.
- [10] M. Moher, "An iterative multiuser decoder for near-capacity communications," *IEEE Transactions on Communications*, vol. 46, no. 7, pp. 870–880, July 1998.
- [11] V. Ramon and L. Vandendorpe, "Predicting the performance and convergence behavior of a turbo-equalization scheme," in *IEEE International Conference on Acoustics, Speech and Signal Processing, ICASSP*, Philadelphia (PA), USA, 2005, vol. 3, pp. 709–712.
- [12] T. Richardson and R. Urbanke, "The capacity of low density parity-check codes under message passing decoding," *IEEE Transactions on Information Theory*, vol. 47, pp. 599–618, Feb. 2001.
- [13] A. Dejonghe and L. Vandendorpe, "Bit-interleaved turbo equalization over static frequency-selective channels : constellation mapping impact," *IEEE Transactions on Communications*, vol. 52, no. 12, pp. 2061–2065, Dec. 2004.